



## Synthesis, Characterization and Adsorption Properties of Protonated Cross-linked Chitosan for the Removal of Basic Blue 3 Dye from Wastewater

<sup>1</sup>\*Chadi, A. S., <sup>2</sup>Saidu, U., <sup>3</sup>Mamman, S. and <sup>1</sup>Abubakar, A. A.

<sup>1</sup>Department of Chemistry, Bauchi State University, Gadau. Nigeria

<sup>2</sup>Department of Chemistry, Sule Lamido University, Kafin-Hausa, Jigawa State, Nigeria.

<sup>3</sup>Department of Chemistry, Nasarawa State University, Keffi. Nigeria.

\*Correspondence Email: abchadis@gmail.com

### ABSTRACT

Dye wastewater remediation is important for water treatment and adsorption is an effective treatment process. A modified protonated crosslinked chitosan (PCCH) was synthesized and compared with pure chitosan for a cationic basic blue 3 dye removal from an aqueous solution. Adsorbent were characterized using techniques such as SEM/EDX, FTIR, and BET analysis. Batch experiments were conducted under optimized pH, adsorbent dosage and initial concentration at room temperature within a range of one hour. The highest adsorption efficiency was 91.93% and 58.97%, adsorption capacity 6.19 mg/g and 3.83 mg/g for PCCH and pure chitosan respectively. Result however fitted well with Langmuir isotherm and pseudo-second-order kinetics models ( $R^2 > 0.99$ ).

**Keywords:** Adsorbent, Adsorption, Basic Blue 3, Chitosan, Crosslinking, Wastewater

### INTRODUCTION

Water pollution is majorly caused by industrial effluents containing different types of synthetic dyes such as basic blue 3 (BB3) which exhibited low biodegradability due to its complex chemical structure and high molecular weight. Over  $10 \times 10^5$  tons of approximately 10,000 different pigments and dye types were reported to have been used in industries annually world-wide as hydrating agent, food colour, pharmaceutical agent, paper, fabrics (Erdal & Taskin, 2010; Nagpal *et al.*, 2010). These dyes and pigments have adverse effects on life in the aquatic environment and subsequently to the mankind through the food chain. The Basic dyes are considered as one of the most toxic substances which causes eye burns which may be responsible for permanent injury to the eyes of human and animals, difficulty in breathing may be sustained by its inhalation, while ingestion through the mouth produces a burning sensation and may cause nausea, vomiting, profuse sweating, mental confusion and methemoglobinemia (Tan *et al.*, 2007, Chu & Chen, 2002). Moreover, these dyes are attributed to increase in water pH and salinity, chemical oxygen demand (COD) and lower the biological oxygen demand (BOD) due to their stability to oxidizing agents, light and resistance to aerobic digestion thereby leading to aquatic plant growth inhibition due to impaired photosynthesis for their utilisation (Ling & Mohd, 2017). Therefore, industrial effluents have become a concern for

significant environmental safety by researchers. Governmental and non-governmental institutions now focus on developing a sustainable design to establish remediation processes to have alternative tracks in addressing wastewater decontamination.

Adsorption, photochemical degradation, reverse osmosis, chemical oxidation, membrane filtration, coagulation–flocculation, aerobic and anaerobic biological degradation are some of the conventional dye removal methods used (Chatterjee *et al.*, 2010). Due to simplicity in design and operation, flexibility, efficiency, less-cost effectiveness and insensitivity in toxic pollutants, adsorption is regarded as more convenient process for removal of dye from wastewater (Benavente, 2008). Many attempts have been made to adsorb pollutants with low cost adsorbents such as activated carbon, clay mineral, cassava peel, date pits, bagasse, olive stones were used by different researchers for dye adsorption (Tan *et al.*, 2007). However, one of the significant problems associated with agricultural adsorbents is production of other secondary pollutants to the water (Yang *et al.*, 2013).

Chitosan (Fig. 1) is a natural polysaccharide polymer that is obtained as a product of the partial chitin deacetylation (Ilyina *et al.*, 2000). Chitosan is the second most abundant biopolymer after cellulose which is a linear heteropolysaccharide compound that consist of a  $\beta$  (1→4) linked to two monosaccharides D-glucosamine and N-acetyl-D-glucosamine (Gul *et al.*

al., 2016). Chitosan primarily consist of three functional groups such as an amino group at C-2, primary and secondary hydroxyl groups at C-3 and C-6 respectively (Ruihua *et al.*, 2017). However, Chitosan naturally exist in the exoskeleton of sea creatures such as shrimps, krill, prawns, crabs, cartilages of molluscs and insect cuticles (Drahansky *et al.*, 2016). It has diverse applications in pollutants remediation with significant performance in every characteristic and desired nature. It is suitable for use due to its environmentally friendly, inexpensive, nontoxicity, biodegradable and biocompatibility nature (Naseeruteen, *et al.* 2018). Moreover, it has some limitations such as solubilities in acidic

medium, low thermal resistance, less mechanical and chemical strength (Zhu *et al.*, 2010, Naseeruteen *et al.*, 2018). Nevertheless, a review data shows its surface chemistry and other features were customised to suit its applications (Terzopoulou *et al.*, 2015). Therefore, the purpose of the present study is to modify chitosan by protonation after cross linkage as adsorbent for the adsorption of BB3 as a dye model, which based on our knowledge there is no record of this work in the literature. The PCCH was characterised to investigate its potential applications. The effects of initial dye concentration and phase contact time on the adsorbent was studied through the batch method of analysis.

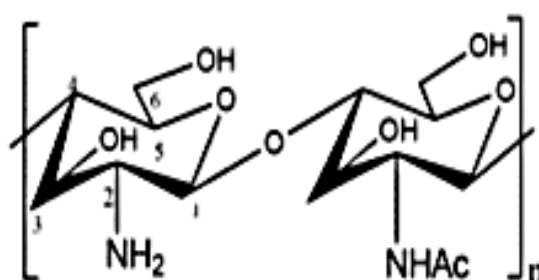


**Figure 1.** Structure of chitosan.

## MATERIALS AND METHODS

### Chemicals and reagents

Chitosan (deacetylation 100%; MW  $2.0 \times 10^5 \text{ g mol}^{-1}$ ), Basic blue 3, hydrochloric acid (HCl), sodium hydroxide (NaOH), sodium nitrate ( $\text{NaNO}_3$ ), potassium bromide (KBr), epichlorohydrin (ECH) and acetic acid ( $\text{C}_2\text{H}_4\text{O}_2$ ) were purchased from Sigma–Aldrich. Ultrapure water for aqueous solutions preparation was obtained by a Millipore purification unit. All chemicals and reagents were of analytical grade and were used without further purification.

### Preparation of Cross-linked chitosan beads (CCH)

The CCH beads was prepared as reported by Wu *et al.*, (2009) and Chiou & Li, (2003) with some modifications. 10g chitosan was added into 300 mL of 30% acetic acid and heated up to  $60^\circ\text{C}$  in a water bath for 1 h. The solution was left overnight to form beads and sieved to constant size after been air dried. 15 mL/g epichlorohydrin (ECH) cross linker was added into 1g solution of the beads in an ultrapure water and shaken at  $60^\circ\text{C}$  for 5 h. The pH of the solution was maintained at 7 in the cross linkage medium.

### Preparation of protonated cross-linked chitosan beads (PCCH)

To protonate the amino groups of the CCH to achieve effective adsorption of BB3 dye, 1g CCH was treated by stirring with 3 mL of 0.5 M HCl for 45 min. Thereafter, the product was neutralized by washing with ultrapure water and dried over night at room temperature for further use (Jaafari *et al.*, 2001). All further experiments were performed with PCCH and the pure chitosan for comparison.

## Characterization

### Instrumental Characterisation

The surface morphology of the derived adsorbent was analysed by scanning electron microscopy (SEM) and energy dispersion x-ray (EDX) was determined with gold coating to make the sorbents electrically conductive for analysis by use of Fei quanta FeG 650 model. Fourier transform infrared (FT-IR) spectra were obtained on a Perkin Elmer system 2000 FT-NIR spectrometer with KBr pellet in the range of  $4000\text{--}400 \text{ cm}^{-1}$ . The Brunauer-Emmett-Teller (BET) method was used for analysis of average pore diameter and surface area, which were measured

through N<sub>2</sub> sorption analysis at 105°C overnight using ASAP 2020 Micromeritics instrument.

### Surface charge characterization (pH point of zero charge (pH<sub>pzc</sub>))

The surface charge of the samples were analysed according to the method reported by Ofomaja & Ho, (2008). 0.1g of the samples were added into 30 mL of 0.1M NaNO<sub>3</sub> solution and shaken at 250 rpm for 24 h to determine the change in pH which was ranged from pH 2-10 and adjusted using 1-0.1M HCl and 1-0.1M NaOH. Subsequently a plot of changes in pH against the initial pH was used to determine the pH<sub>pzc</sub>.

### Batch Adsorption Experiments

A solution of 100 mg/L was prepared by dissolving 0.10g of BB3 dye into 1 L of ultrapure water to prepare the stock in a set of Erlenmeyer flasks and a series of 10 – 50 mg/g initial concentrations were made from the stock. 20mL aliquot solution of BB3 were shaken with both adsorbents separately for an hour to reach equilibrium concentration using orbital shaker, then the dye concentrations at room temperature were determined before and after shaking using UV-VIS spectrometer at 654 nm. The adsorption capacity (q<sub>e</sub>) and removal percentage of BB3 were calculated using equations 1 and 2 respectively (Chu & Chen, 2002).

$$q_e = \frac{[(C_0 - C_e)]}{m} \times V \quad (1)$$

$$R (\%) = \frac{m}{C_0} \times 100 \quad (2)$$

where C<sub>0</sub> and C<sub>e</sub> (mg/L) are the concentrations of BB3 before sorption and at equilibrium time, respectively, V (mL) is the volume of solution and m (g) is the weight of the adsorbent.

Effects of contact time, pH and initial dye concentration on the BB3 sorption on sorbents at room temperature were determined by the batch technique. 0.02g of the sorbents were added into 10 mg/L of the dye at different contact time (10-60 min.), and a range of pH (2-10). The supernatant were taken to measure equilibrium phase concentrations of dye using UV-VIS spectrometer at time t which was presented as q<sub>t</sub> (mg/g) as a calculated value (Yan *et al.*, 2013). However, 0.02 g to 0.1 g were used to measure the effects of sorbent dosage within 60 min.

## RESULTS AND DISCUSSION

### SEM/EDX measurements

Surface morphology of the pure chitosan and PCCH was determined using SEM/EDX analysis and the results are presented in Fig. 2a and 2b, respectively. As can be seen from Fig. 2a, pure chitosan has a rough and symmetrical surface, whereas the surface of the PCCH (Fig. 2b), was coarser and asymmetrical, probably due to the addition of chloride ions on the pure chitosan. To further confirm the formation of PCCH, EDX analysis was conducted and the result is presented in Fig. 2c. As can be seen from the EDX result, there is the presence of C, O, N and Cl, an evidence of loading chloride ions on the pure chitosan which resulted in the formation of PCCH.

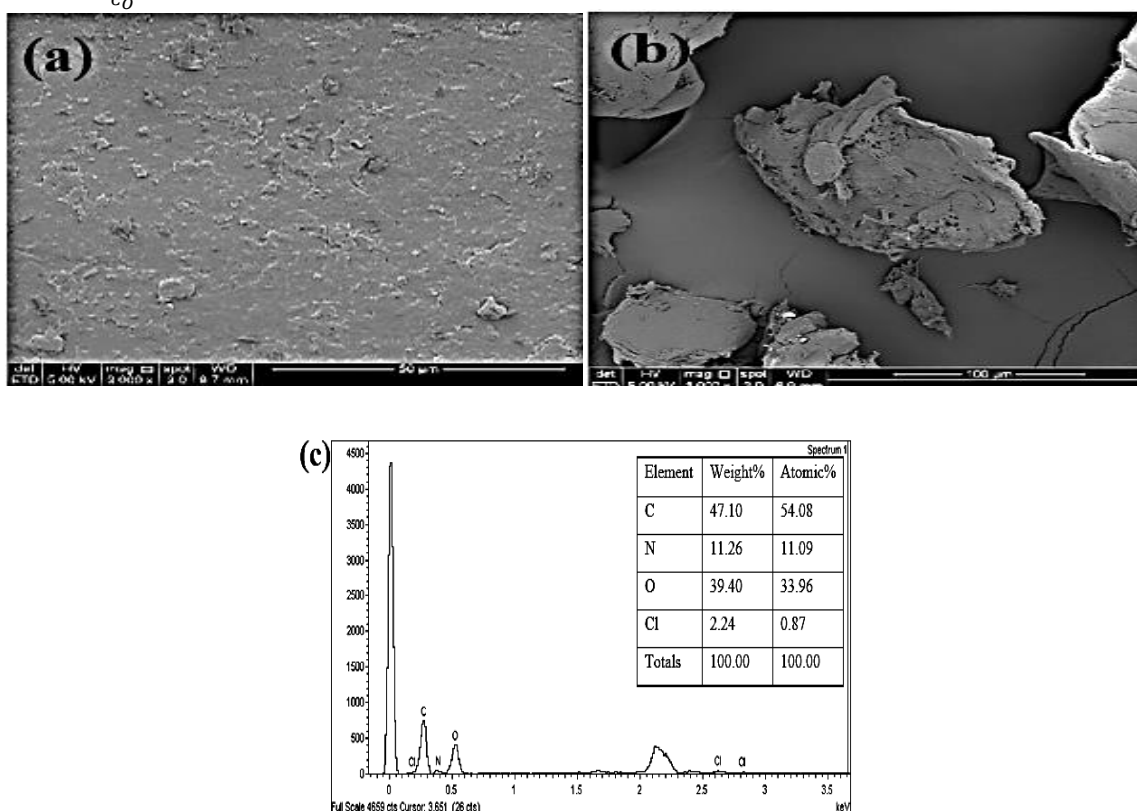


Figure 2 SEM images of (a) Pure chitosan (b) PCCH and the (c) EDX graph of PCCH

### BET Measurements

The surface area and pore size of the pure chitosan and PCCH were analysed using BET method and the results are presented in Table 1. As presented on the table, the pore sizes of pure chitosan and PCCH are 3.594 nm and 51.9279 nm, respectively. However, International Union of Pure and Applied Chemistry (IUPAC) classified pore

sizes into micropores ( $d < 2$  nm), mesopores ( $2 < d < 50$  nm), and macropores ( $d > 50$  nm) (Wan & Hanafiah, 2008). Moreover, the BET surface area of pure chitosan increased from 2.45  $\text{m}^2/\text{g}$  to 8.75  $\text{m}^2/\text{g}$  in PCCH. Increase in the surface area of an adsorbent facilitates more adsorption of pollutants, hence, PCCH is expected to give higher adsorption compared to pure chitosan.

**Table 1.** BET Results of Pure Chitosan and PCCH Adsorbents

Adsorbent	BET Surface Area ( $\text{m}^2/\text{g}$ )	Langmuir Surface Area ( $\text{m}^2/\text{g}$ )	Pore Diameter (nm)
Pure Chitosan	2.45	3.27	3.594
PCCH	8.75	12.24	51.928

### Fourier Transform Infrared (TF-IR) analysis

The FTIR spectra of the pure chitosan and PCCH before and after adsorption are presented in Fig. 3a -d. As can be seen from the spectra of pure chitosan before and after adsorption figure 3a and 3b respectively, the band at 3104 to 3132  $\text{cm}^{-1}$  correspond to stretching vibration of O-H. NH stretching vibration is located to 1654  $\text{cm}^{-1}$ . The band at 1401 – 1399  $\text{cm}^{-1}$  correspond to  $\text{CH}_2\text{OH}$  stretching in chitosan. A peak for CN stretching is at 1321 – 1311  $\text{cm}^{-1}$ , CO stretching vibration in COH is assigned at 1086 – 1075  $\text{cm}^{-1}$ . The spectra

of PCCH before adsorption is presented in Fig. 3c, appearance of a new absorption band at 1566  $\text{cm}^{-1}$  due to interaction of  $\text{NH}_2$  with Cl established crosslinking and protonation had taken place. -C-O-C corresponds to an asymmetric stretching vibration at 1075 – 1057  $\text{cm}^{-1}$  (Elsabee & Morsi, 2009). However, the peak shifted to lower absorption band 1547  $\text{cm}^{-1}$  after dye adsorption as shown in Fig. 4d. but, since there is no observed new peak on both adsorbents after adsorption, confirmed that the adsorption process is merely an ionic or physical interaction (Kaur *et al.*, 2019).

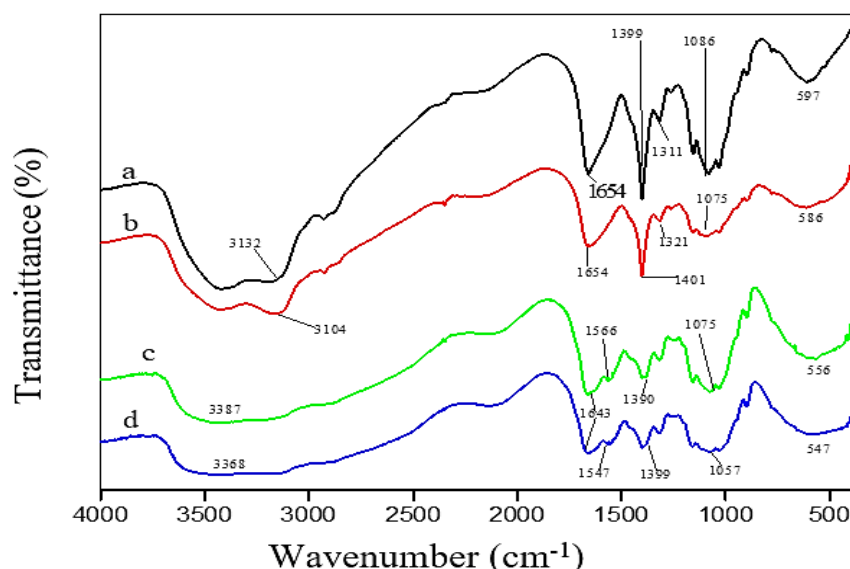


**Figure 3.** FTIR spectra for (a) Pure chitosan, (b) Pure chitosan after adsorption of BB3 (c) PCCH and (d) PCCH after adsorption of BB3.

### pH point of zero charge ( $\text{pH}_{\text{pzc}}$ )

The pH point of zero charge ( $\text{pH}_{\text{pzc}}$ ) is generally described as the pH at which the net charge of adsorbent's surface is equal to zero in an aqueous solution during sorption of ionic species (Irfan *et al.*, 2015). In this work, a plot for  $\text{pH}_{\text{pzc}}$  determination of the pure chitosan and PCCH are shown in Figure 4a and b respectively. From the results, the  $\text{pH}_{\text{pzc}}$  of the pure chitosan is 6.77, while that of PCCH is 3.92. Therefore, the result

indicated that sorption of cationic dye would be more noticeable at lower pH due to lower ionic interaction competition between the ions on the sorbents surface and the dye (Huang *et al.*, 2019). Moreover, pH below  $\text{pH}_{\text{zpc}}$  is indicated that the surfaces of the adsorbents is positively charged and above the  $\text{pH}_{\text{zpc}}$  is negatively charged due to accumulation of  $\text{H}^+$  ions from the bulk to surround the adsorbents surfaces (Lu *et al.*, 2012).

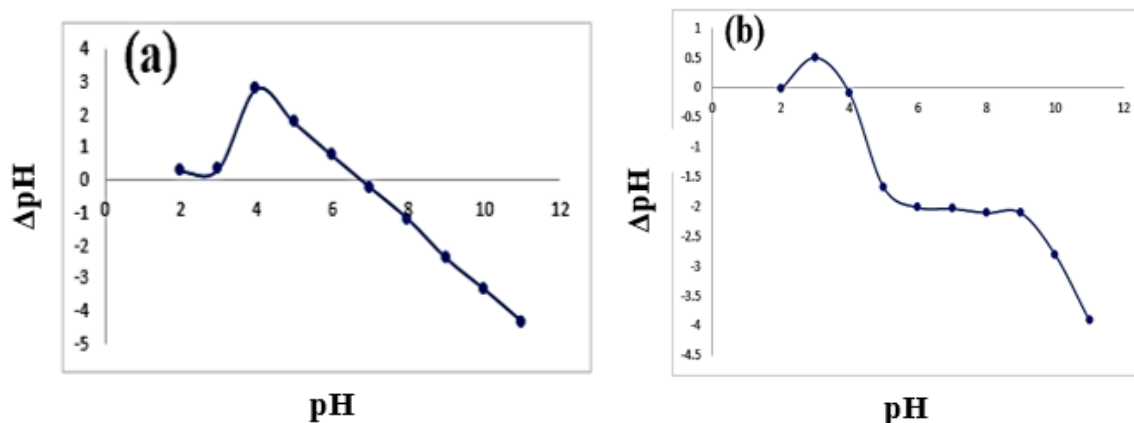


Figure 4. pH<sub>pzc</sub> of (a) Pure chitosan and (b) PCCH adsorbents

## BATCH ADSORPTION STUDIES

### Effect of pH

A range of pH 2-10 were studied at a constant concentration for pure chitosan and PCCH as shown in Fig5 a and b respectively. Maximum percent removal was recorded at pH 4 for both adsorbents due to less competition of H<sup>+</sup> interaction at lower pH with the dye, less inhibition of ions by electrostatic interaction and chitosan surface protonation. However, there is decrease in negatively charged adsorbent sites and increase in the positively charged site this cause attraction between the NH<sub>2</sub> group and the charge species of dye. But a dramatic change due to the chemistry of the dye, cationic molecular nature of the dye and

the adsorbent surface pH<sub>pzc</sub> have much influences on the trend of sorption process (Özer *et al.*, 2006). At pH 4 the surface was positively charged, and the cationic dye molecule was repelled at the surface due to the competition between the cations and protons, hence, resulted in low adsorption of BB3 at low pH. Similar results were reported by other researchers (Saha *et al.*, 2010; Auta & Hameed, 2014; Zhang and Guo, 2014). The removal percentage recorded is up to 38.08% and 89.77% for pure chitosan and PCCH respectively. Meanwhile, the adsorption of BB3 through electrostatic attraction was facilitated in the PCCH adsorbent due dominant negative charges on its surface (Zhang *et al.*, 2014).

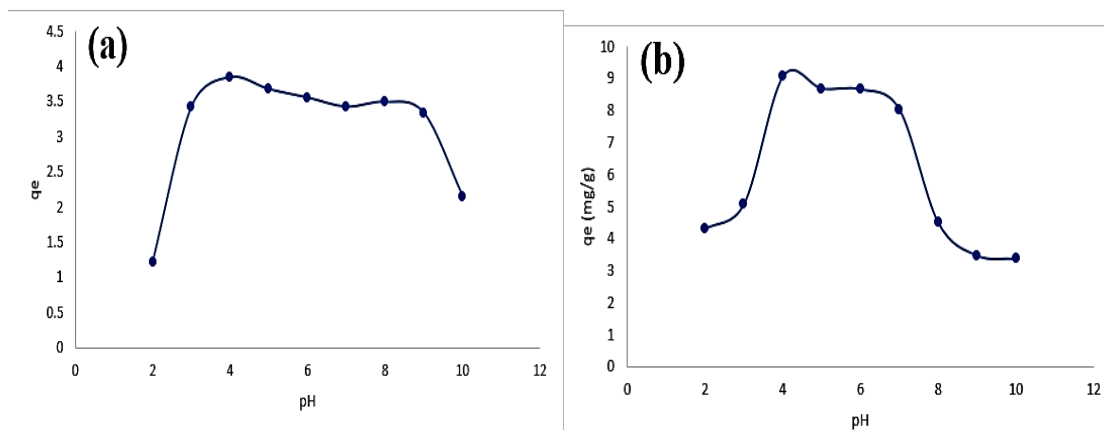
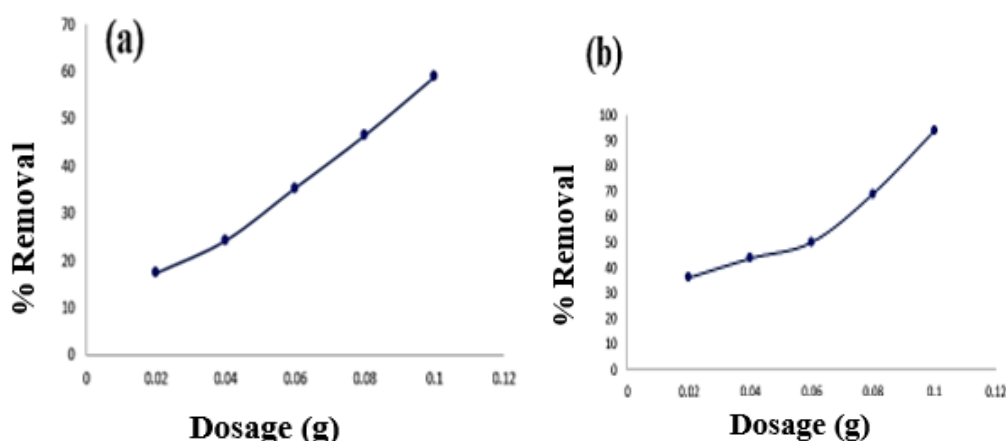


Figure 5. Effect of pH on a) Pure chitosan and b) PCCH adsorbents

### Effect of adsorbents dosage

The function of number of available sites for adsorption of adsorbent is justified by the available surface area for adsorption (Naseeruteen *et al.*, 2018). Fig. 6a and b, shows the removal efficiency increases with increased in dosage from 0.02 g to 0.1 g in both pure chitosan and PCCH adsorbents respectively. This is due to an increase in the availability of active binding sites on the adsorbent surface. However, the adsorption

capacity which is the amount of BB3 adsorbed per unit weight decreased with increasing adsorbent dosage due to saturation of adsorption sites. Pure chitosan decreases from 3.50 mg/g to 2.37 mg/g, likewise adsorption capacity of PCCH was observed from 7.25 mg/g to 3.76. Contrary, the percent removal was increased up to 58.98 % from 17.40 % and 36.25 % to 93.95 % respectively for pure chitosan and PCCH respectively.



**Figure 6.** Effect of (a) Pure chitosan and (b) PCCH dosage on BB3 removal

### Effect of contact time and kinetics of adsorption

Figure 7 (a) and (b) show the effect of contact time on the adsorption of BB3 by pure chitosan and PCCH adsorbent respectively. Obviously, during the first 20 minutes, the adsorption performance was good, equilibrium was achieved within 60 minutes. This is attributed to the active site exposure for reactivity in sorption and large surface area of the sorbents. Sorption was so rapid at the initial stages and then followed gradually in the process due to decrease in the active bonding sites on the adsorbents and increased between particulates aggregation.

The kinetics of BB3 adsorption was studied in order to understand the behaviour of sorbents. Adsorption at time intervals were studied with the pseudo-first-order model and is expressed mathematically by equation 3.

$$\log(q_e - qt) = \log q_e - \frac{k_1 t}{2.303} \quad (3)$$

Where  $qt$  and  $q_e$  (mg/g) are the amounts of the BB3 adsorbed at equilibrium and time  $t$ ,  $k_1$  (1/min) is the rate constant of the pseudo-first-order sorption. Usually pseudo-first order is a linear plot of  $\log(q_e - qt)$  against time.

The kinetics data obtained for BB3 adsorption by sorbents was applied to the pseudo-second order kinetic model as well, following the linear form of model as given in equation 4.

$$\frac{t}{qt} = \frac{1}{k_2 q_e^2} + \frac{t}{q_e} \quad (4)$$

$$qt = k_p t^{1/2} + C \quad (5)$$

Where  $k_2$  is the values of rate constants and  $q_e$  is the amount adsorbed at equilibrium, determined from the slopes and intercepts of a linear plot of  $q/t$  against time respectively and is shown in Table 2.

The plot is used to know the rate determining or controlling step and prediction of

behaviour over the whole range of time with chemisorption mechanism of adsorption is also studied by the pseudo second-order model (Naseeruteen *et al.*, 2018). In this work however, the correlation coefficient clearly shows agreement with pseudo second order model (0.9986 and 0.9907) for adsorption of pure chitosan and PCCH respectively. This suggest that the rate limiting process of adsorption in this work might be a physisorption. However, Correlation coefficient ( $R^2$ ) to check the validity of the models with the experimental and calculated data value indicated pseudo-second-order was higher than the pseudo-first-order for both adsorbents, but the calculated equilibrium adsorption capacity agreed better with the pseudo-first-order as indicated in table 2. This indicated that the adsorption was valid to be predicted with pseudo-first-order and supported the assumption that the pseudo-first-order adsorption kinetics is supported at the initial stage of the porous adsorbents adsorption process (Zhu *et al.*, 2010, Luo & Zhang, 2009, Demirbas, Dizge, Sulak, & Kobya, 2009).

Intraparticle diffusion model was computed from a linear plot of  $qt$  against  $t^{0.5}$ . Obtained from a plot of equation 5 where  $k_p$  and  $C$  are the intraparticle diffusion rate constant (mg/g min<sup>1/2</sup>) and the intercept for the intraparticle diffusion model (mg/g) respectively. Represented on Table 2. It is sorts to establish sequences of dye adsorption (i.e. BB3 molecules migrates towards pure chitosan and PCCH surface by film diffusion) at faster rate and the second stage is film diffusion on the boundary layer of pure chitosan and PCCH. Finally a gradual uptake of the dye through intraparticle diffusion take place through ion exchange, complexation or chelation onto the active sites of adsorbents (Nandi, 2009). Nevertheless, diffusion is controlled by dye migration of its liquid phase, external film resistance or intraparticle resistance, subject to size of molecule of the dye (Weber, 1963).

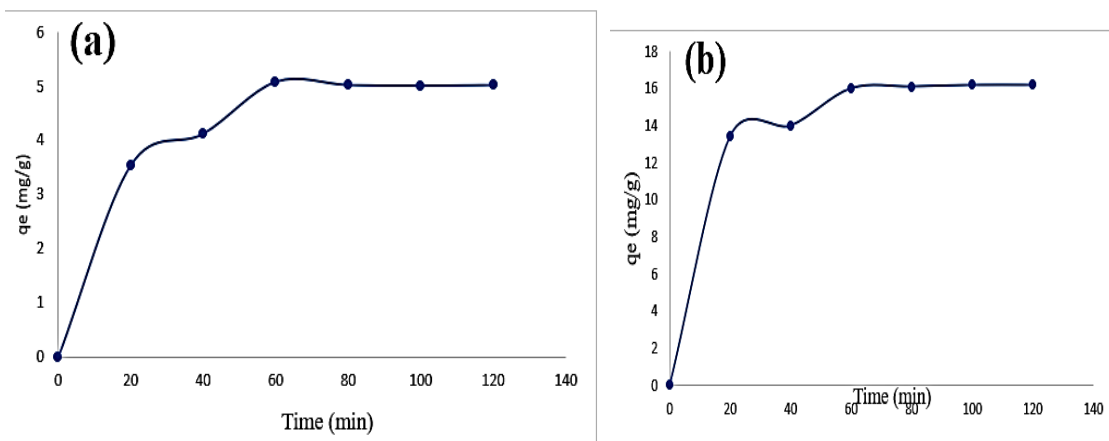


**Figure 7.** Effect of contact time on (a) Pure chitosan and (b) PCCH

### Equilibrium Adsorption Isotherms.

Adsorption of dye is expressed by a sorbent relation at a particular temperature per unit mass (Tang & Zhang, 2015). Adsorption capacity for BB3 was studied with Langmuir isotherm model expressed mathematically in equation 6 as follows:

$$\frac{C_e}{q_e} = \frac{1}{Q_b} + \frac{C_e}{Q} \quad (6)$$

Where a linear plot of  $C_e/q_e$  against  $C_e$  for sorption of BB3 was used from linear and intercept to obtain the maximum sorption capacity ( $q_m$ ) and constant of binding energy ( $R_L$ ) shown in Table 3. It is indicated that correlation coefficients ( $R^2$ ) based on the Langmuir isotherm model fitted well with the BB3 adsorption on both sorbents (0.9904 and 0.9961) for PCCH and the pure chitosan respectively. Moreover, a dimensionless factor of separation  $R_L$  using equation 7 shows that the calculated value correlated to the BB3 adsorption were found at less than unity as presented in Table 3. However, in all cases for BB3 adsorption shows that Langmuir model is found to be favourable to describe the process.

A Freundlich linear equation was applied to relate data for BB3 adsorption is presented mathematically in equation (8).

$$R_L = \frac{1}{1+bC_0} \quad (7)$$

$$\log q_e = \log K_f + \frac{1}{n} \log C_e \quad (8)$$

$$q_e = \frac{RT}{bT} \ln kT + \frac{RT}{bT} \ln ce \quad (9)$$

From the intercept and slopes, the values of  $n$  and  $K_F$  were respectively calculated. As somewhere reported (Rajesh *et al.*, 2010), adsorption process is validated as favourable or unfavourable by this relationship, that adsorption is favourable if  $0.1 < 1/n < 1$ . Besides, it is unfavourable if  $1/n > 2$ . Therefore, adsorption is favourable for both sorbents as the values of  $1/n$  are less than one. There are number of reported works that shows applicability of dyes adsorption which fitted well to Freundlich and or Langmuir adsorption isotherm models (Uzun & Güzel, 2005; Huang *et al.*, 2019; Fan *et al.*, 2012). However, Langmuir adsorption isotherm is the most appropriate model to describe the adsorption process in this work.

Temkin adsorption isotherm equation 9 is used to study direct interaction effect between adsorbates and heat of adsorption of all molecular layer interactions, it assumes that the interaction decreases linearly due to interaction coverage (Demirbas *et al.*, 2009). The constants  $KT$  and  $bT$  obtained from linear plot of  $q_e$  against  $\ln C_e$  indicated the correlation coefficient  $R^2$  obtained was 0.9236 shown in table 3 it is quite high but is not the best model to describe the process in this work.

**Table 2:** Kinetic parameters for BB3 adsorption on Pure chitosan and PCCH adsorbents

Model	Parameter	Pure chitosan	PCCH
Pseudo-first-order	qe exp. (mg/g)	3.84	6.19
	qe cal (mg/g)	3.7	6.14
	k1 (min)	0.0479	0.4698
	R <sup>2</sup>	0.2471	0.4412
Pseudo-second-order	qe cal (mg/g)	4.39	6.98
	k2 (min)	0.0265	0.0164
	h (mg/g min)	0.511	0.8004
	R <sup>2</sup>	0.9986	0.9907
Intraparticle diffusion	qe cal (mg/g)	10.07	11.07
	k2 (mg/g min)	0.2314	0.3289
	c (mg/g)	2.0975	3.5763
	R <sup>2</sup>	0.9596	0.9142

**Table 3.** Constants of adsorption isotherms for BB3 adsorption on pure and PCCH adsorbents

Model	Parameter	Pure chitosan	PCCH
Langmuir	qm (mg/g)	31.06	19.92
	b (L/mg)	0.0332	0.6363
	R <sub>L</sub>	0.0310	0.0311
	R <sup>2</sup>	0.9961	0.9904
Freundlich	qm (mg/g)	1.43	3.86
	k <sub>F</sub> (mg/g)	1.49	8.73
	n <sub>F</sub>	0.671	0.115
	R <sup>2</sup>	0.9873	0.7328
Temkin	K <sub>T</sub> (L/mg)	4.48	12.35
	b <sub>T</sub> (KJ/mol)	170.43	712.36
	R <sup>2</sup>	0.9236	0.7715

## CONCLUSION

A PCCH was successfully prepared and used for BB3 adsorption. PCCH possessed higher adsorption capacity than the pure chitosan. Adsorption capacity was found to increase as the initial concentration were increased and decreased at above pH 4. Batch adsorption experiment and kinetics reveal that the processes were fitted well with Langmuir and pseudo-second-order isotherm model. This work showed that PCCH composite has potentials for clean-up applications as a good and efficient adsorbent for different environmental pollutants.

## REFERENCES

Auta, M., & Hameed, B. H. (2014). Chitosan-clay composite as highly effective and low-cost adsorbent for batch and fixed-bed adsorption of methylene blue. *Chemical Engineering Journal*, 237, 352–361. <https://doi.org/10.1016/j.cej.2013.09.066>

Chatterjee, S., Lee, M. W., & Wooa, S. H. (2010). Adsorption of congo red by chitosan hydrogel beads impregnated with carbon nanotubes. *Bioresource Technology*, 101(6), 1800–1806. <https://doi.org/10.1016/j.biortech.2009.10.051>

Chiou, M. S., & Li, H. Y. (2003). Adsorption behavior of reactive dye in aqueous solution on chemical cross-linked chitosan beads. *Chemosphere*, 50(8), 1095–1105. [https://doi.org/10.1016/S0045-6535\(02\)00636-7](https://doi.org/10.1016/S0045-6535(02)00636-7)

Chu, H. C., & Chen, K. M. (2002). *Reuse of activated sludge biomass I. Removal of basic dyes from.pdf*. 37, 595–600.

- Demirbas, E., Dizge, N., Sulak, M. T., & Kobya, M. (2009). Adsorption kinetics and equilibrium of copper from aqueous solutions using hazelnut shell activated carbon. *Chemical Engineering Journal*, 148(2–3), 480–487. <https://doi.org/10.1016/j.cej.2008.09.027>
- Drahansky, M., Paridah, M. ., Moradbak, A., Mohamed, A. ., Owolabi, F. abdulwahab taiwo, Asniza, M., & Abdul Khalid, S. H. . (2016). We are IntechOpen , the world ' s leading publisher of Open Access books Built by scientists , for scientists TOP 1 % . *Intech*, i(tourism), 13. <https://doi.org/http://dx.doi.org/10.5772/57353>
- Erdal, S., & Taskin, M. (2010). Uptake of textile dye Reactive Black-5 by *Penicillium chrysogenum* MT-6 isolated from cement-contaminated soil. *African Journal of Microbiology Research*, 4(8), 618–625.
- Fan, L., Luo, C., Sun, M., Li, X., Lu, F., & Qiu, H. (2012). Preparation of novel magnetic chitosan/graphene oxide composite as effective adsorbents toward methylene blue. *Bioresource Technology*, 114, 703–706. <https://doi.org/10.1016/j.biortech.2012.02.067>
- Gul, K., Sohni, S., Waqar, M., Ahmad, F., Norulaini, N. A. N., & A. K., M. O. (2016). Functionalization of magnetic chitosan with graphene oxide for removal of cationic and anionic dyes from aqueous solution. *Carbohydrate Polymers*, 152, 520–531. <https://doi.org/10.1016/j.carbpol.2016.06.045>
- Huang, P., Xia, D., Kazlauciuonas, A., Thornton, P., Lin, L., & Menzel, R. (2019). Dye-Mediated Interactions in Chitosan-Based Polyelectrolyte/Organoclay Hybrids for Enhanced Adsorption of Industrial Dyes. *ACS Applied Materials and Interfaces*, 11(12), 11961–11969. <https://doi.org/10.1021/acsami.9b01648>
- Ilyina, A. V., Tikhonov, V. E., Albulov, A. I., & Varlamov, V. P. (2000). Enzymic preparation of acid-free-water-soluble chitosan. *Process Biochemistry*, 35(6), 563–568. [https://doi.org/10.1016/S0032-9592\(99\)00104-1](https://doi.org/10.1016/S0032-9592(99)00104-1)
- Irfan Shah, R.A., Wan Saime Wan Ngah, N. M. (2015). Iron Impregnated Activated Carbon as an Efficient Adsorbent for the Removal of Methylene Blue: Regeneration and Kinetics Studies. *PLoS ONE*, 10(4), 1-23.
- Jaafari, K., Elmaleh, S., Coma, J., & Benkhouja, K. (2001). Equilibrium and kinetics of nitrate removal by protonated cross-linked chitosan. *Water SA*, 27(1), 9–13.
- Kaur, K., Jindal, R., & Meenu. (2019). Self-assembled GO incorporated CMC and Chitosan-based nanocomposites in the removal of cationic dyes. *Carbohydrate Polymers*, 225(July), 115245. <https://doi.org/10.1016/j.carbpol.2019.115245>
- L. Zhang, H.Z., W. Guo, Y. T. (2014). Removal of malachite green and crystal violet cationic dyes from aqueous solution using activated sintering process red mud. *Appl. Clay Sci.*, 93–94, 85–93.
- Ling, Y. Y., & Mohd Suah, F. B. (2017). Extraction of malachite green from wastewater by using polymer inclusion membrane. *Journal of Environmental Chemical Engineering*, 5(1), 785–794. <https://doi.org/10.1016/j.jece.2017.01.001>
- Lu, X., Jiang, J., Sun, K., Xie, X., & Hu, Y. (2012). Surface modification, characterization and adsorptive properties of a coconut activated carbon. *Applied Surface Science*, 258(20), 8247–8252. <https://doi.org/10.1016/j.apsusc.2012.05.029>
- Luo, X., & Zhang, L. (2009). High effective adsorption of organic dyes on magnetic cellulose beads entrapping activated carbon. *Journal of Hazardous Materials*, 171(1–3), 340–347. <https://doi.org/10.1016/j.jhazmat.2009.06.009>
- M.Z. Elsabee, R.E. Morsi, A. M. A.-S. (2009). Surface active properties of chitosan and its derivatives. *Colloids Surf., B* 74, 1–16.
- Martha Benavente, T. (2008). Adsorption of Metallic Ions onto Chitosan: Equilibrium and Kinetic Studies,. In *Royal Institute of Technology*. Sweden.
- Nagpal, K., Singh, S. K., & Mishra, D. N. (2010). Chitosan nanoparticles: A promising system in novel drug delivery. *Chemical and Pharmaceutical Bulletin*, 58(11), 1423–1430. <https://doi.org/10.1248/cpb.58.1423>
- Nandi BK, G.A., P. M. (2009). Adsorption characteristics of Brilliant Green dye on kaolin. *J Hazard Mater.*, 161, 387–395.
- Naseeruteen, F., Hamid, N. S. A., Suah, F. B. M., Ngah, W. S. W., & Mehamod, F. S. (2018a). Adsorption of malachite green from aqueous solution by using novel chitosan ionic liquid beads. In *International Journal of Biological Macromolecules* (Vol. 107). <https://doi.org/10.1016/j.ijbiomac.2017.09.111>

Naseeruteen, F., Hamid, N. S. A., Suah, F. B. M., Ngah, W. S. W., & Mehamod, F. S. (2018b).

- Adsorption of malachite green from aqueous solution by using novel chitosan ionic liquid beads. *International Journal of Biological Macromolecules*, 107(PartA), 1270–1277. <https://doi.org/10.1016/j.ijbiomac.2017.09.111>
- Ofomaja, A. E., & Ho, Y. S. (2008). Effect of temperatures and pH on methyl violet biosorption by *Mansonia wood* sawdust. *Bioresource Technology*, 99(13), 5411–5417. <https://doi.org/10.1016/j.biortech.2007.11.018>
- Özer, A., Akkaya, G., & Turabik, M. (2006). The removal of Acid Red 274 from wastewater: Combined biosorption and biocoagulation with *Spirogyra rhizopus*. *Dyes and Pigments*, 71(2), 83–89. <https://doi.org/10.1016/j.dyepig.2005.06.004>
- Rajesh Kannan, R., Rajasimman, M., Rajamohan, N., & Sivaprakash, B. (2010). Equilibrium and kinetic studies on sorption of malachite green using *Hydrilla Verticillata* biomass. *International Journal of Environmental Research*, 4(4), 817–824.
- Ruihua Huang, Qian Liu, Jie Huo, B. Y. (2017). *Huang2017.pdf* (pp. 24–32). pp. 24–32. <https://doi.org/org/10.1016.jarabjc.2013.05017>
- Saha, P., Chowdhury, S., Gupta, S., & Kumar, I. (2010). Insight into adsorption equilibrium, kinetics and thermodynamics of Malachite Green onto clayey soil of Indian origin. *Chemical Engineering Journal*, 165(3), 874–882. <https://doi.org/10.1016/j.cej.2010.10.048>
- Tan, I. A. W., Hameed, B. H., & Ahmad, A. L. (2007). Equilibrium and kinetic studies on basic dye adsorption by oil palm fibre activated carbon. *Chemical Engineering Journal*, 127(1–3), 111–119. <https://doi.org/10.1016/j.cej.2006.09.010>
- Tang, B., H. Zhang, and K. H. R. (2015). Application of deep eutectic solvents in the extraction and separation of target compounds from various samples biomedicine. *J. Food and Environment*, 38, 1053–1064.
- Terzopoulou, Z., Kyzas, G. Z., & Bikiaris, D. N. (2015). Recent advances in nanocomposite materials of graphene derivatives with polysaccharides. *Materials*, 8(2), 652–683. <https://doi.org/10.3390/ma8020652>
- Uzun, I., & Güzel, F. (2005). Rate studies on the adsorption of some dyestuffs and p-nitrophenol by chitosan and monocarboxymethylated(mcm)-chitosan from aqueous solution. *Journal of Hazardous Materials*, 118(1–3), 141–154. <https://doi.org/10.1016/j.jhazmat.2004.10.006>
- Wan Ngah, W. S., & Hanafiah, M. A. K. M. (2008). Removal of heavy metal ions from wastewater by chemically modified plant wastes as adsorbents: A review. *Bioresource Technology*, 99(10), 3935–3948. <https://doi.org/10.1016/j.biortech.2007.06.011>
- Weber WJ Jr, M. J. (1963). Kinetics of adsorption on carbon from solution. *J Sanit Eng Div Am Soc Civil Eng.*, 89, 31–60.
- Wu, Y., Wang, Y., Luo, G., & Dai, Y. (2009). In situ preparation of magnetic Fe<sub>3</sub>O<sub>4</sub>-chitosan nanoparticles for lipase immobilization by cross-linking and oxidation in aqueous solution. *Bioresource Technology*, 100(14), 3459–3464. <https://doi.org/10.1016/j.biortech.2009.02.018>
- Yan, Y., Xiang, B., Li, Y., & Jia, Q. (2013). Preparation and adsorption properties of diethylenetriamine-modified chitosan beads for acid dyes. *Journal of Applied Polymer Science*, 130(6), 4090–4098. <https://doi.org/10.1002/app.39691>
- Yang, H., Li, Y., Ho, S. S. H., Tian, X., Xia, Y., Shen, Y., ... Pan, G. (2013). Preparation and characterization of EDTA-modified magnetic-Fe<sub>3</sub>O<sub>4</sub> chitosan composite: Application of comparative adsorption of dye wastewater with magnetic chitosan. *Water Science and Technology*, 68(1), 209–216. <https://doi.org/10.2166/wst.2013.217>
- Zhang, L., Zhang, H., Guo, W., & Tian, Y. (2014). Removal of malachite green and crystal violet cationic dyes from aqueous solution using activated sintering process red mud. *Applied Clay Science*, 93–94, 85–93. <https://doi.org/10.1016/j.clay.2014.03.004>
- Zhu, H. Y., Jiang, R., Xiao, L., & Li, W. (2010). A novel magnetically separable  $\gamma$ -Fe<sub>2</sub>O<sub>3</sub>/crosslinked chitosan adsorbent: Preparation, characterization and adsorption application for removal of hazardous azo dye. *Journal of Hazardous Materials*, 179(1–3), 251–257. <https://doi.org/10.1016/j.jhazmat.2010.02.087>